PHYSICAL REVIEW C VOLUME 8, NUMBER 4 OCTOBER 1973

Neutron Polarization from $^2H(p,\vec{n})$ and $^1H(d,\vec{n})$†

F. N. Rad,* L. C. Northcliffe, D. P. Saylor, J. G. Rogers,‡ and R. G. Graves
Cyclotron Institute, Texas A&M University, College Station, Texas 77843
(Received 2 July 1973)

Measurements of the neutron polarization in the $p-d$ breakup reaction are reported. The polarization of breakup neutrons from $^2H(p,\vec{n})$ has been measured at $E_p = 21.4$ MeV, $\theta_{lab} = 18°$, as a function of neutron energy with an accuracy of approximately ±0.01. The measurement is consistent with zero from 8 to 13 MeV, but shows a small but significant positive polarization from 14 to 18 MeV. A similar measurement of the breakup neutrons from the $^1H(d,\vec{n})2p$ reaction at the same center-of-mass momentum ($E_d = 42.8$ MeV), also at $\theta_{lab} = 18°$, shows nonzero polarization over the neutron energy region 8 to 25 MeV, reaching a maximum of about -0.05 ± 0.01. In both cases, the polarization of the breakup neutrons is opposite in sign to that expected if the dominant process is simple quasifree scattering.

I. INTRODUCTION

The three-body problem has been the subject of vigorous theoretical attack during the past decade. Observables which have been calculated include the differential cross section, vector and tensor polarizations for elastic scattering, and inelastic differential cross sections. Exact three-body calculations by Aaron, Amado, and Yam,[1] and by Sloan,[2] using the Faddeev-Lovelace equations[3] with simple S-wave separable N-N potentials have given good agreement with the experimental elastic N-d differential cross sections for medium and low energies. However, because of the restriction to S-wave forces these calculations could not give the observed polarizations and it was clear that calculations with more realistic N-N potentials would be required to fit such data. Pieper and Kowalski[4] and Aarons and Sloan[5] then extended three-body calculations to include the effects of the D-state component of the deuteron. These calculations predicted nonzero vector and tensor polarizations in N-d elastic scattering but the predictions of vector polarizations did not resemble the experimental data with which they were compared. More recent calculations by Doleschall[6] using both P-wave potentials and S-D coupling, and by Pieper[7] using complete P-wave and S-wave potentials along with S-D coupling have produced good fits to the N-d data in the elastic channel. Thus it has been demonstrated in the case of elastic scattering that polarization data provide an important test of any calculation which strives to be more realistic than one using an S-wave separable potential.

It seems likely that the measurement of polarization parameters for the breakup channel will be of similar value and prove to be a stimulant to theory and a test of new theoretical results. It also is reasonable to expect that the breakup reaction will be more sensitive to the combined effect of off-energy-shell and three-body forces than is N-d elastic scattering.[8]

This paper reports measurements of the polarization of the breakup neutrons as a function of neutron energy at $\theta_{lab} = 18°$ from p-d collisions at 14.3 MeV in the center-of-mass system. Both the $^1H(d,\vec{n})$ and $^2H(p,\vec{n})$ reactions were studied, corresponding to observation of the breakup neutrons at different center-of-mass angles. A brief account of some of these results has already been given.[9]

II. EXPERIMENTAL METHOD

The beam of unpolarized hydrogen or deuterium ions, accelerated by the Texas A&M variable energy cyclotron, was energy-analyzed and directed through a high-pressure liquid-nitrogen-cooled gas target in the experimental area (see Fig. 1). The target cell had entrance and exit windows of 2.5-cm diameter covered by Havar foils of 25-μm thickness which were sealed to the window frames with epoxy cement. The cell thickness was 6.4 cm, giving an areal density of 1.84×10^{22} atoms/cm^2 at the operating pressure of 15 atm. The energy loss in the target gas was 1.69 MeV for both beams and the mean energy in the gas was 21.4 MeV for protons and 42.8 MeV for deuterons. Immediately after the target the beam was deflected magnetically through 90° and collected by a heavily shielded Faraday cup.

The liquid-helium polarimeter was positioned 4.5 m from the target on a collimated line at 18° laboratory angle. The polarimeter consisted of a liquid-helium scattering sample of volume 154 cm^3 surrounded by four NE102 plastic scintillators placed at scattering angles of 78° and 125° to left and right of the scatterer. Each NE102 detector subtended a solid angle of 0.061 sr and was located 41 cm from the liquid-helium cell. These two scattering angles were chosen because the analyzing

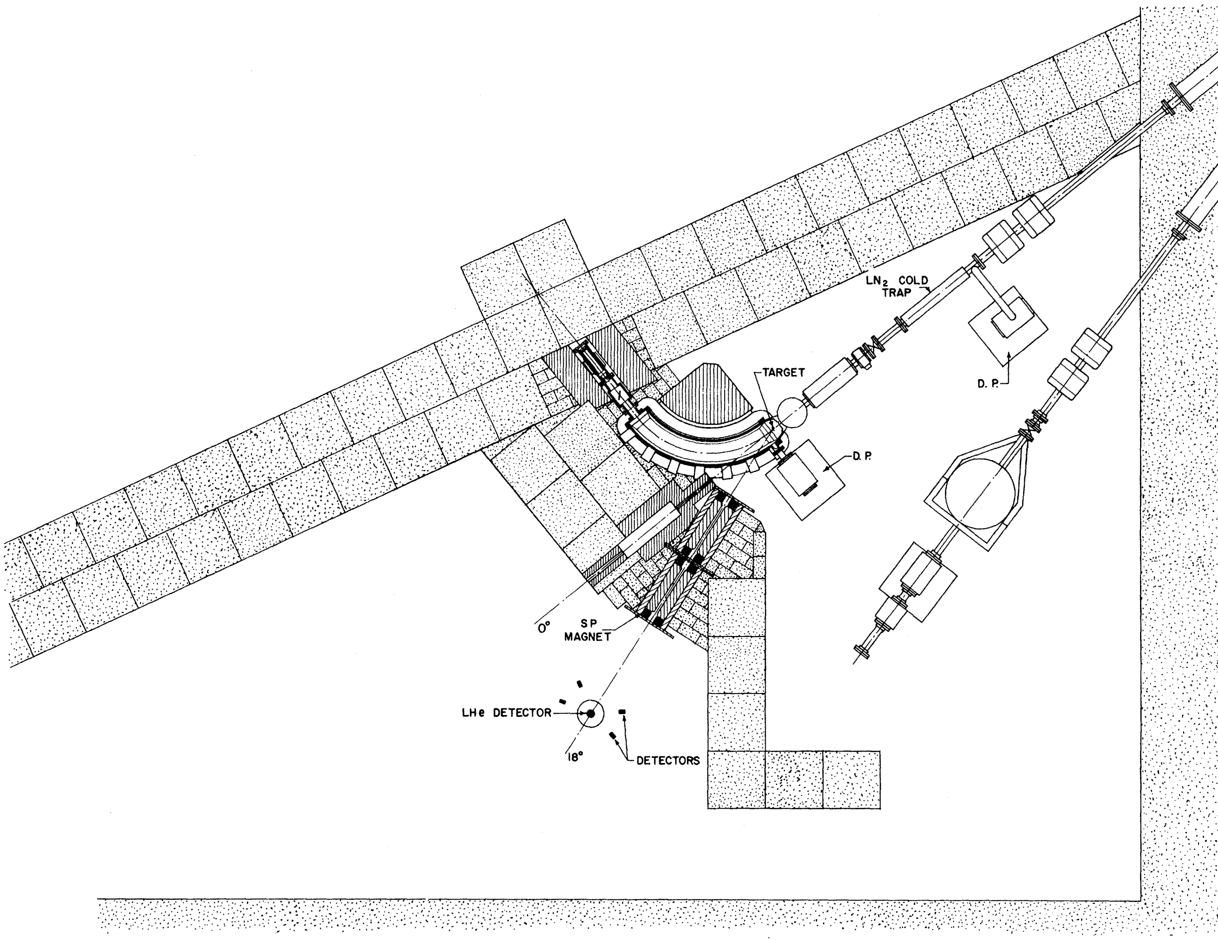

FIG. 1. Over-all view of the experimental area showing location of the neutron production target, the liquid N_2 cold trap, the 90° sweep magnet, the Faraday cup, the beam-dump shielding, the two spin-precession (SP) magnets positioned in tandem on the line at $\theta_{lab} = 18°$, and the position of the liquid-helium polarimeter.

power of helium is large for both but opposite in sign over the entire neutron energy region studied. The scattered-neutron detectors were viewed by RCA-8575 photomultiplier tubes through light pipes of length 7.6 cm polished for maximum internal reflection and also tapered to 4.6 cm (the photocathode diameter). The scintillations caused by the recoil helium ions were viewed by a RCA-7326 photomultiplier tube, through a light pipe 7.6 cm in length. To minimize false asymmetries due to local variations in room background and to efficiency and geometry differences of the left and right scattered-neutron detectors, a pair of transverse-field spin-precession magnets were placed in tandem in the 18° line to precess the spin of neutrons incident on the polarimeter by ~180° on alternate runs. All photomultiplier tubes were shielded from stray magnetic fields by Netic-Conetic magnetic shielding. The neutrons were collimated, in part, by the pole gaps of the two magnets. The polarimeter and the neutron detectors were isolated from the background flux from the target and beam dump by a concrete shielding wall 2 m in thickness, as shown in Fig. 1. The facility and apparatus are discussed in more detail elsewhere.[10,11]

For each experiment, runs were made with the polarities of the spin-precession magnets alternately antiparallel (symbolized $\uparrow$) in which case there was no net precession of neutron spins, and then parallel (symbolized $\downarrow$) in which case the spin of 19.8-MeV neutrons was precessed by 180°. (The precession angle ranged from 286° for 7.6-MeV neutrons to 145° for 30.8-MeV neutrons.) Background runs, viz. empty target runs, were also taken with magnets alternately in the ($\uparrow$) and ($\downarrow$) configuration.

The data were acquired with an on-line computer. Five parameters were stored for each event, and written event by event on magnetic tape for later off-line analysis. Figure 2 shows a simplified block diagram of the electronic apparatus used. The five parameters extracted from the electronic system were: (t), the time of flight from target to helium cell; (δt), the time of flight from helium cell to plastic scintillator; (H), the pulse height from the helium cell; (h), the pulse height from the plastic scintillator; a tag word to indicate which of the four scattered-neutron detectors produced a pulse. The NE102 inputs to the AND module were stretched to a duration of 300 nsec so that δt values derived from signals from adjacent beam bursts (separated by ~94 nsec) could be observed and used to determine the accidental coincidence contribution to the data. The helium linear signals were amplified. The threshold of each of the plastic detector discriminators was set on the Compton edge of the spectrum from ^{60}Co γ rays. The threshold settings were noncritical since more accurate digital thresholds could be set during the computer analysis of the data.

The primary flux monitor was the integrated beam current collected during the run by the dump Faraday cup; this current was corrected for multiple-scattering losses by comparison with a Faraday cup upstream of the target. Secondary electron emission in the dump Faraday cup was suppressed through use of an electrostatic guard ring and a magnetic field.

Independent bases for determining the relative normalization of different runs was provided by a series of scalers which recorded the singles counts in the helium and plastic detectors, the coincidence count between the helium and plastic detectors, and the number of computer strobes. The difference between the latter two also served as a measure of the integrated dead time.

III. DATA ANALYSIS

The methods used in the off-line analysis of the multiparameter data are discussed in detail elsewhere[10,12] and will be described here only briefly. The neutron energy was determined from the time of flight between the production target and the helium cell, calibrated by observing γ-rays from the target in the time spectrum of helium cell singles counts.[13] Corrections for discriminator time walk in all detectors were found to be important for clearer separation of certain background events from the true events and were made before extraction of the asymmetry values. This is demonstrated in Fig. 3, which shows the number of counts versus δt for all of the ($\uparrow$) runs for neutrons from the ^{1}H($d, \vec{n}$)2p reaction detected with the 125° left detector. Curve (a) shows the raw δt spectrum. The real coincidence events are confined to the large peak in this spectrum, which has a width due to differing scattered-neutron velocities, beam-pulse time resolution, detector time walk, and finite detector dimensions. Curve (b) shows the δt spectrum corrected for the broadening due to the different scattered neutron velocities and to discriminator walk, both in the helium and the plastic neutron-detector timing signals. The true events are seen to fall in a narrow peak [full width at half maximum (FWHM) = 3.3 nsec, consistent with the geometrical resolution], which is clearly resolved from a second peak of time-correlated background events. The origin of this background has not yet been determined, but the clear separation of the two peaks makes possible the elimination of these false

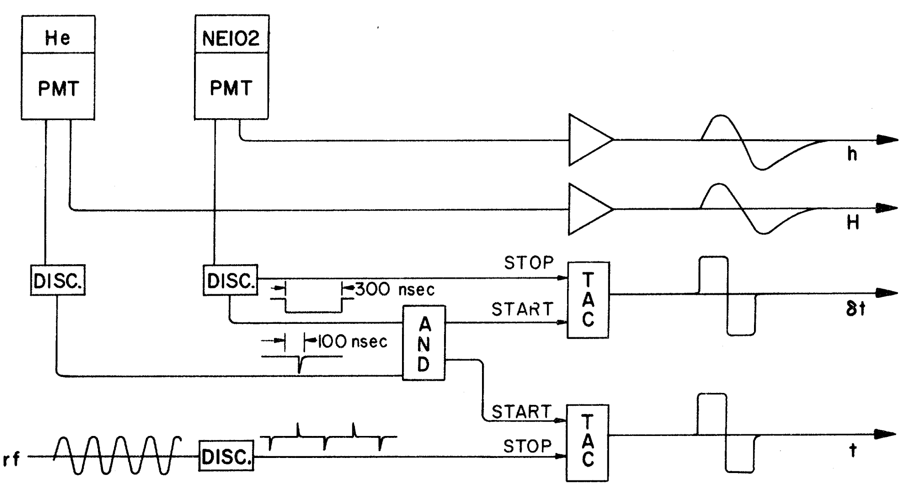

FIG. 2. Block diagram for neutron-polarization electronics, greatly simplified.

events by use of a single channel gate on the δt value, as shown in the figure.

The other types of backgrounds might be expected from accidental coincidences arising from the neutron flux down the 18° line and from the ambient flux of neutrons and γ rays in the experimental area. The presence of the first type would be indicated by a peak on the δt plot separated from the true peak by one cyclotron rf period. There was no evidence of such background in either the ^{2}H(p, $\vec{n}$)2p or the ^{1}H(d, $\vec{n}$)2p data. The background arising from ambient flux is indicated by events falling between the true peak and the expected position of the above mentioned false peak. Such background showed no time structure and was negligible in comparison with the true event rate.

One further source of background was the spectrum of neutrons produced in the Havar windows of the target, which was investigated by making runs with no gas in the target. While this background made a negligible contribution to the ^{2}H(p, $\vec{n}$)2p data it amounted to about 7% in the ^{1}H(d, $\vec{n}$)2p data and is shown by curve (c) of Fig. 3. This background exhibited no measurable asymmetry but was sufficiently large to make background subtraction necessary.

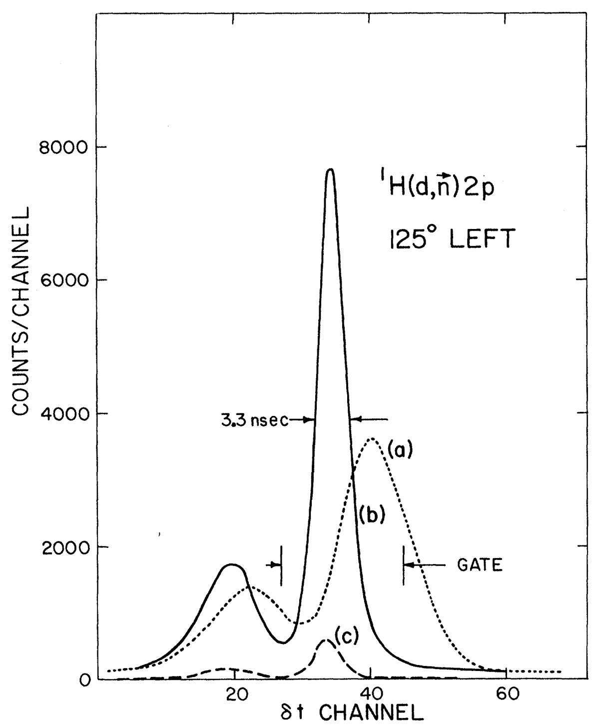

FIG. 3. The distribution of time intervals (δt) between signals from the helium cell and the 125° left plastic scintillator for the ^{1}H(d, $\vec{n}$) reaction. Curve (a): raw δt distribution; curve (b): distribution of δt after removal of contributions due to "time walk" both in the He discriminator signal and the NE102 discriminator signal, and for velocity differences of the scattered neutrons; curve (c): background neutrons from the Havar windows. The gate is explained in the text.

In the ensuing discussion the asymmetry $\epsilon(E_n)$ is defined to be the product $\epsilon(E_n) = P(E_n)a(E_n)$ of the incident-neutron polarization $P_n(E_n)$ and the n-He analyzing power $a(E_n)$, both for neutron energy E_n. The asymmetry values for the ^{2}H(p, $\vec{n}$) breakup neutrons were obtained by summing all of the ($\uparrow$) and ($\downarrow$) runs of unrejected data for each detector separately with proper normalization (as determined by the total singles counts recorded in the He cell for each run) and using the formula

$$\epsilon(E_n) = \frac{N\uparrow - N\downarrow}{N\downarrow - \cos(\phi) N\uparrow}, \tag{1}$$

where $N\uparrow$ and $N\downarrow$ are the total number of counts for neutrons of energy E_n for ($\uparrow$) and ($\downarrow$) runs, respectively, and ϕ is the calculated neutron-precession angle for neutrons of energy E_n in the ($\downarrow$) case. The error was calculated using the equation

$$\Delta = \frac{1 - \cos\phi}{(N\downarrow - N\uparrow \cos\phi)^2} (N\downarrow^2 N\uparrow + N\uparrow^2 N\downarrow)^{1/2}. \tag{2}$$

Errors calculated with Eq. (2) were in agreement with errors calculated by compounding the standard deviations of individual ($\uparrow$) and ($\downarrow$) runs. For the extraction of asymmetry values in the ^{1}H(d, $\vec{n}$) reaction it was necessary to modify Eqs. (1) and (2) appropriately to take the background subtraction into account.

Since four-parameter data were accumulated simultaneously with four scattered-neutron detectors, many internal consistency checks were possible. For a given E_n, the asymmetry values

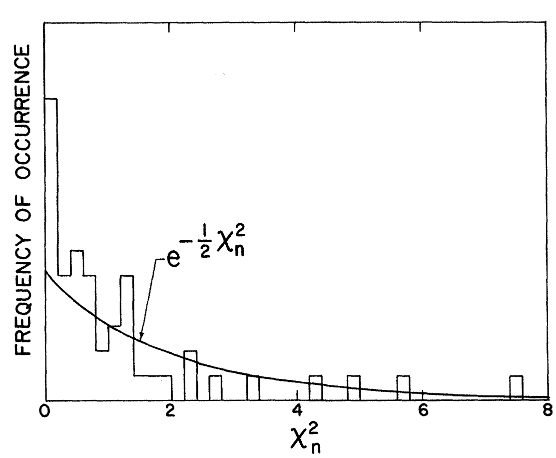

FIG. 4. Distribution of values of χ^2_n as defined in the text. The smooth curve is expected if the distribution of deviations between left and right asymmetry determinations is a normal distribution.

determined from (↑) and (↓) runs with each detector for any two of the four parameters could readily be checked with those determined with the other detectors. For example, the asymmetries $\epsilon_L(E_n)$ determined using left detectors and those $\epsilon_R(E_n)$ determined using right detectors should agree. That is $\chi^2_n = [\epsilon_L(E_n) - \epsilon_R(E_n)]^2/[\Delta_L{}^2(E_n) + \Delta_R{}^2(E_n)] \approx 1$. More precisely, the values of χ^2_n should be distributed as $e^{-\chi^2_n/2}$. Figure 4 shows this distribution for the 125° detectors from the $^1H(d,\vec{n})$ experiment compared with $e^{-\chi^2_n/2}$ normalized to the number of energy bins. The agreement is seen to be good, which indicates that the distribution of deviations is in agreement with expectations based on the theory of statistics. A further check on the asymmetry values extracted by the above methods was made by comparing them with the left-right asymmetry calculated directly, and the agreement was good. Thus it seems probable that the errors are primarily statistical.

The neutron polarization $P_n(E_n) = \epsilon(E_n)/a(E_n)$ was computed from $\epsilon(E_n)$ and the n-^{4}He analyzing power $a(E_n)$ using values of $a(E_n)$ computed from the set of smooth curves hand drawn through the phase-shift sets of Hoop and Barschall,[14] Satchler *et al.*,[15] Stammbach and Walter,[16] and Broste *et al.*[17] shown in Fig. 5. The calculated polarizations are shown in Figs. 6 and 7 for the $^2H(p,\vec{n})2p$ and the $^1H(d,\vec{n})2p$ reactions, respectively.

The energy binning has been made approximately equal to the average energy loss of the beam in the target. No corrections for finite-geometry effects in the polarimeter have been included, since a Monte Carlo calculation[18] of the finite geometry and the multiple-scattering effects in the polarimeter showed that those corrections were always much smaller than the statistical uncertainties.

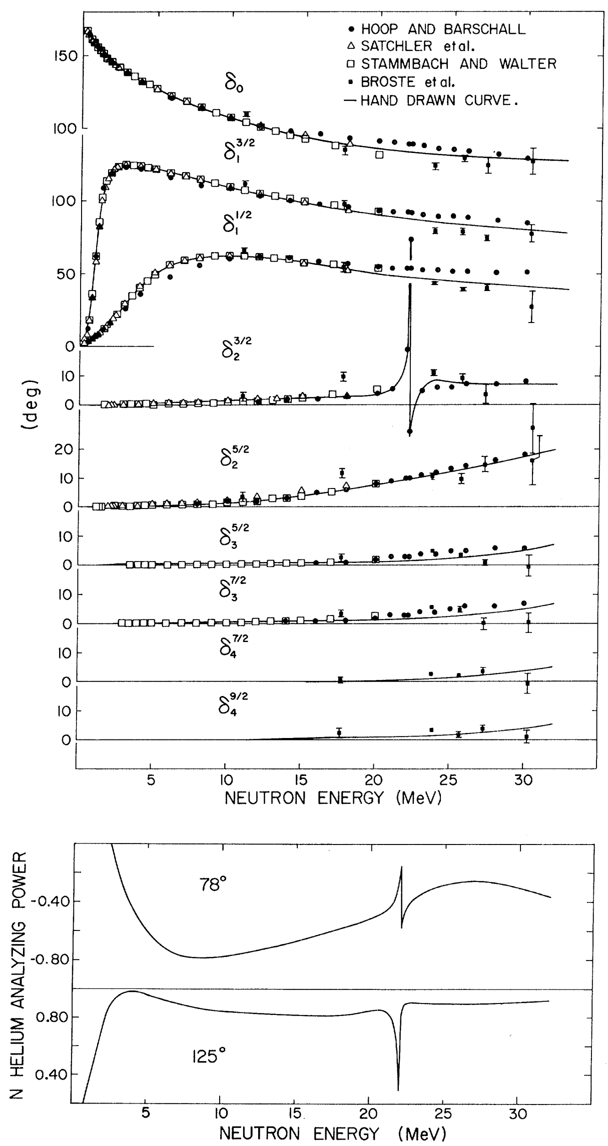

FIG. 5. Calculated n-^{4}He analyzing power and the smooth curves hand drawn through the phase-shift sets of Hoop and Barschall (Ref. 14), Satchler *et al.* (Ref. 15), Stammbach and Walter (Ref. 16), and Broste *et al.* (Ref. 17).

IV. RESULTS AND DISCUSSION

For the $^2H(p,\vec{n})$ reaction at $E_p = 21.4$ MeV the measured neutron polarization (Fig. 6) is definitely positive in the 13–18 MeV region and peaks to about 0.02 ± 0.01. For the $^1H(d,\vec{n})$ reaction at $E_d = 42.8$ MeV the measured neutron polarization (Fig. 7) is larger but negative and peaks to about -0.05 ± 0.01. In both cases the observed neutron polarization clearly differs from the zero value given by the Amado model.[1,19]

It might be hoped that the nonzero neutron polarization could be explained in terms of quasifree n-p scattering (QFS) since a simple calculation

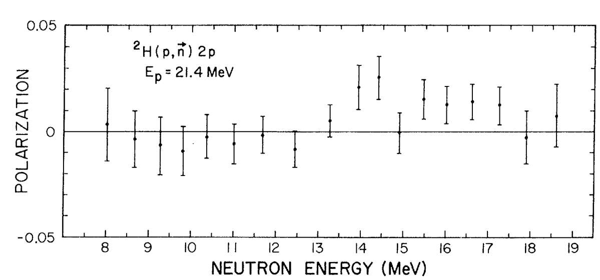

FIG. 6. The polarization (P_n) of the neutrons from $^2H(p,\vec{n})2p$ at $E_p = 21.4$ MeV as a function of the neutron energy obtained by combining all data. The error bars show the statistical standard deviation of the measurement, which appears to be the principal uncertainty.

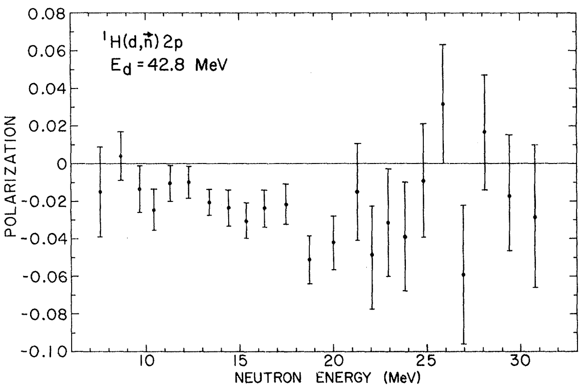

FIG. 7. The polarization (P_n) of the neutrons from $^1H(d,\vec{n})2p$ at $E_d = 42.8$ MeV as a function of neutron energy obtained by combining all data. The error bars show the statistical standard deviation of the measurement, which appears to be the principal uncertainty.

would predict the QFS contribution to be a broad peak in the neutron energy spectrum, centered at an energy which agrees approximately with that of the observed polarization maximum in both reactions. In fact, the magnitude of the polarization observed in this region for both reactions is close to the value expected if n-p QFS provides the dominant contribution to the cross section there. In both cases, however, the sign of the observed polarization is opposite to that expected for QFS.

In the $^2H(p, \vec{n})$ reaction the neutron is a component of the target, and knockout of the neutron at a small angle to the left by the incident proton is equivalent to neutron scattering at a large angle (~144° c.m.) to the right. Thus the positive polarization parameter observed in free n-p scattering corresponds to downward polarization (i.e., a negative polarization parameter) for the $^2H(p, \vec{n})$ reaction, according to the Basel convention.[20]

In the $^1H(d, \vec{n})$ reaction the neutron is a component of the incident particle, and an outgoing neutron at $\theta_{\text{lab}} = 18°$ to the left corresponds to n-p QFS, also at small angle to the left (~36° c.m.). In this case, according to the convention, the sign of the polarization should be the same for $^1H(d, \vec{n})$ neutrons as for free n-p scattering, if n-p QFS is the dominant breakup mechanism.

The values expected for the free n-p polarization are about +0.015 at $\theta_{\text{c.m.}} = 144°$ and +0.05 at $\theta_{\text{c.m.}} = 36°$, according to both the Yale IV[21] and MacGregor, Arndt, and Wright (MAW X)[22] energy-dependent phase-shift analyses. The validity of the polarization values derived from these phase-shift sets is supported by an n-p polarization measurement at 23.1 MeV.[23] A comparison of these values with the peak polarizations seen in Figs. 6 and 7 shows that, in each case, the predicted and observed polarizations agree in magnitude but are opposite in sign. It is natural to suspect the existence of a sign error in the analysis, but extensive checking has only reaffirmed the correctness of the sign. Independent support for the correctness of the sign is provided by the fact that during one of the polarization runs a measurement was made of the neutron polarization in the $^2H(d, \vec{n})^3He$ reaction, as a check on procedures. The result obtained, $P = +0.075 \pm 0.006$ at $E_d = 15.2$ MeV, is in good agreement with the previous measurement of Hardekopf, *et al*.[24]

Thus far, none of our efforts to find a simple explanation of the observed polarizations (especially their signs) have been successful. Perhaps this is not surprising since, as pointed out by Amado and Rubin,[25] the multiple-scattering series is not convergent or at best is only slowly convergent at low energies. This indicates that predictions based on QFS cannot be reliable. It is also unlikely that any single reaction mechanism such as QFS or a final-state interaction completely dominates a kinematically incomplete measurement. It seems likely that methods such as those used by Doleschall[6] and Peiper[7] must be applied before the polarization of nucleons from low-energy N-d breakup can be understood.

ACKNOWLEDGMENT

We are grateful for the assistance of Dr. M. Jain and Dr. J. D. Bronson, and particularly M. L. Evans. We would also like to express our sincere thanks to Dr. H. E. Conzett of the Lawrence Berkeley Laboratory and Dr. J. F. Reading and Dr. Judith Binstock for interesting discussions of the results and of possible polarization-producing mechanisms.

†Work supported in part by the National Science Foundation. Based in part on the Ph.D. dissertation of F. N. Rad, Dept. of Physics, Texas A&M University, 1973 (unpublished).

*Present address: Lawrence Berkeley Laboratory, University of California at Berkeley, Berkeley, California.

‡Present address: Nuclear Research Center, University of Alberta, Edmonton, Alberta, Canada.

[1]R. Aaron, R. D. Amado, and Y. Y. Yam, Phys. Rev. 140, B129 (1965).

[2]I. H. Sloan, Phys. Rev. 185, 1361 (1969); Nucl. Phys. A168, 211 (1971).

[3]L. D. Faddeev, Zh. Eksp. Teor. Fiz. 39, 1459 (1960)

[transl.: Sov. Phys.-JETP 12, 1014 (1961)]; C. Lovelace, Phys. Rev. 135, B1225 (1964).
[4]S. C. Pieper and K. L. Kowalski, Phys. Rev. C 5, 306 (1972).
[5]J. C. Aarons and I. H. Sloan, Nucl. Phys. A182, 369 (1972).
[6]P. Doleschall, Phys. Lett. 38B, 298 (1972); 40B, 443 (1972).
[7]S. C. Pieper, Nucl. Phys. A193, 529 (1972); and in *Proceedings of the International Conference on Few Particle Problems in the Nuclear Interaction, Los Angeles, California, 1972,* edited by (North-Holland, Amsterdam, 1972), pp. 308—313.
[8]D. P. Saylor and F. N. Rad, Phys. Rev. C 8, 507 (1973).
[9]F. N. Rad, L. C. Northcliffe, J. G. Rogers, and D. P. Saylor, Phys. Rev. Lett. 31, 57 (1973).
[10]F. N. Rad, Ph.D. thesis, Department of Physics, Texas A&M University (unpublished).
[11]F. N. Rad, R. G. Graves, L. C. Northcliffe, and D. P. Saylor, to be published.
[12]F. N. Rad, L. C. Northcliffe, and D. P. Saylor, to be published.
[13]L. C. Northcliffe, C. W. Lewis, and D. P. Saylor, Nucl. Instr. Meth. 83, 93 (1970).
[14]B. Hoop, Jr., and H. H. Barschall, Nucl. Phys. 83, 65 (1966).
[15]G. R. Satchler, L. W. Owen, A. J. Elwyn, G. L. Morgan, and R. L. Walter, Nucl. Phys. A112, 1 (1968).
[16]Th. Stammbach and R. L. Walter, Nucl. Phys. A180, 225 (1972).
[17]N. B. Broste, G. S. Mutchler, J. E. Simmons, R. A. Arndt, and L. D. Roper, Phys. Rev. C 5, 761 (1972).
[18]The Monte Carlo program is the one described in W. B. Broste, Los Alamos Scientific Laboratory Report No. LA-4596 (unpublished).
[19]R. Aaron and R. D. Amado, Phys. Rev. 150, 857 (1966).
[20]Nucl. Phys. 21, 696 (1960).
[21]G. Breit, Rev. Mod. Phys. 39, 560 (1967); R. E. Seamon, R. A. Frideman, G. Breit, R. D. Haracz, J. M. Holt, and A. Prakash, Phys. Rev. 165, 1579 (1968).
[22]M. H. MacGregor, R. A. Arndt, and R. M. Wright, Phys. Rev. 182, 1714 (1969).
[23]G. S. Mutchler and J. E. Simmons, Phys. Rev. C 4, 67 (1971).
[24]R. A. Hardekopf, P. W. Lisowski, T. C. Rhea, R. L. Walter, and T. B. Clegg, Nucl. Phys. A191, 468 (1972).
[25]R. D. Amado and M. H. Rubin, Phys. Rev. C 7, 2151 (1973).